

THE PROTO-NEUTRON STAR PHASE OF THE COLLAPSAR MODEL AND THE ROUTE TO LONG-SOFT GAMMA-RAY BURSTS AND HYPERNOVAE

L. DESSART,¹ A. BURROWS,¹ E. LIVNE,² AND C. D. OTT¹

Received 2007 October 30; accepted 2007 December 16; published 2008 January 2

ABSTRACT

Recent stellar evolutionary calculations of massive low-metallicity fast-rotating main-sequence stars yield iron cores at collapse that are endowed with high angular momentum. It is thought that high angular momentum and black hole formation are critical ingredients for the collapsar model of long-soft γ -ray bursts (GRBs). We present two-dimensional multigroup, flux-limited-diffusion MHD simulations of the collapse, bounce, and immediate postbounce phases of a $35 M_{\odot}$ collapsar-candidate model of Woosley & Heger. Provided that the magnetorotational instability (MRI) operates in the differentially rotating surface layers of the millisecond-period neutron star, we find that a magnetically driven explosion occurs during the proto-neutron star phase, in the form of a baryon-loaded nonrelativistic jet, and that a black hole, which is central to the collapsar model, does not form. Paradoxically, although much uncertainty surrounds stellar mass loss, angular momentum transport, magnetic fields, and the MRI, current models of chemically homogeneous evolution at low metallicity yield massive stars with iron cores that may have *too much* angular momentum to avoid a magnetically driven, hypernova-like explosion in the immediate postbounce phase. We surmise that fast rotation in the iron core may inhibit, rather than enable, collapsar formation, which requires a large angular momentum *above* the core but not in it. Variations in the angular momentum distribution of massive stars at core collapse might explain both the diversity of Type Ic supernovae/hypernovae and their possible association with a GRB. A corollary might be that, through its effect on magnetic field amplification, the angular momentum distribution, rather than the progenitor mass, is the distinguishing characteristic of these outcomes.

Subject headings: gamma rays: bursts — MHD — neutrinos — stars: neutron — stars: rotation — supernovae: general

1. INTRODUCTION

There is mounting observational evidence for the association between long-soft γ -ray bursts (GRBs) and broad-lined Type Ic supernovae (SNe; see Woosley & Bloom 2006 for a review). Such hydrogen-deficient (and perhaps also helium-deficient) progenitors are compact, and, if fast-rotating in their cores at collapse, they fulfill the critical requirements for the formation of a collapsar (Woosley 1993). The engine that converts energy from long-term accretion of disk material onto the black hole (BH) may power a relativistic jet in the excavated polar regions. The jet breaks out of the progenitor surface while equatorial accretion continues. Depending on the BH mass and the angular momentum budget in the collapsing envelope, this “engine” may operate for seconds (i.e., as long as a typical long-soft GRB). Accompanying this beamed relativistic polar jet might be a disk wind, fueled by neutrinos or MHD processes that would explode the Wolf-Rayet envelope. This explosion and the radioactive ^{56}Ni material produced might lead to a very energetic, broad-lined, Type Ic SN of the hypernova variety (Iwamoto et al. 1998; MacFadyen & Woosley 1999; Hjorth et al. 2003; Stanek et al. 2003).

State-of-the-art radiation-hydrodynamics simulations, including a sophisticated equation of state (EOS) and a detailed neutrino transport (Buras et al. 2006; Burrows et al. 2006, 2007a; Kitaura et al. 2006; Marek & Janka 2007), suggest that, although the neutrino mechanism for supernova explosions may work for the lower mass massive progenitors, it may not work for the more

massive progenitors, which are characterized by an ever higher postbounce accretion rate onto the proto-neutron star (PNS). Burrows et al. (2006, 2007a) have suggested that an acoustic mechanism will work for all slowly rotating progenitors that do not explode by other means within the first second after bounce. However, massive star cores endowed with large angular momentum at the time of collapse should experience the magnetorotational instability (MRI; Balbus & Hawley 1991; Akiyama et al. 2003; Pessah et al. 2006; Shibata et al. 2006; Etienne et al. 2006), and these cores have the potential to exponentially amplify weak initial fields on a rotation timescale. The saturation values of such fields are ultimately set by the free energy of differential rotation available in the surface layers of the PNS (Ott et al. 2006), and these values can be large (e.g., on the order of 10^{15} G at a radius of a few tens of kilometers). The corresponding magnetic stresses at the neutron star surface can systematically lead to powerful jetlike explosions ~ 100 ms after bounce (see, e.g., Ardeljan et al. 2005; Yamada & Sawai 2004; Kotake et al. 2004; Sawai et al. 2005; Moiseenko et al. 2006; Obergaulinger et al. 2006; Burrows et al. 2007b, hereafter B07; Dessart et al. 2007).

In this Letter, we investigate, in the context of the collapsar model, the potential implications of this magnetic explosion mechanism. Our study focuses on the immediate postbounce phase, whose importance was emphasized by Wheeler et al. (2000, 2002). This is in contrast to previous work that explored only the phase subsequent to BH formation (MacFadyen & Woosley 1999; Aloy et al. 2000; Zhang et al. 2003; Proga 2005). Indeed, the two terms that are sometimes used in the context of collapsars are “failed SN” (MacFadyen & Woosley 1999) and “prompt BH formation” (MacFadyen et al. 2001). Our analysis supports the idea that the conditions for the collapsar model, as stated so far, are also suitable for a magnetically driven explosion in the immediate post-core-bounce PNS

¹ Department of Astronomy and Steward Observatory, University of Arizona, Tucson, AZ 85721; luc@as.arizona.edu, burrows@as.arizona.edu, cott@as.arizona.edu.

² Racah Institute of Physics, Hebrew University, Jerusalem, Israel; eli@frodo.fiz.huji.ac.il.

TABLE 1

PROPERTIES OF TWO MHD-VULCAN/2D SIMULATIONS OF THE 350C
COLLAPSTAR MODEL OF WH06

Model	t_{end} (ms)	t_0 (ms)	M_{10} (M_{\odot})	P_{10} (ms)	E_{expl} (B)	\dot{E}_{gas} ($B \text{ s}^{-1}$)	\dot{E}_{EXB} ($B \text{ s}^{-1}$)	v_{max} (km s^{-1})
(1)	(2)	(3)	(4)	(5)	(6)	(7)	(8)	(9)
M0	369	...	2.1	4	0.03	0.5	0.25	43,000
M1	666	349	1.7	12	3.31	9.4	3.0	58,000

COLUMNS.—(1) The models used; (2) the time at the end of each simulation and (3) the time when the rate of polar mass ejection first overcomes equatorial mass accretion (all quoted quantities in the table correspond to the final time in each simulation, whereas times are given with respect to core bounce); (4) the total baryonic mass and (5) the average rotation period, both inside the $10^{10} \text{ g cm}^{-3}$ isodensity contour; (6) the explosion energy; (7) the Bernoulli power in the ejecta and (8) the Poynting power in the ejecta, both obtained by integrating the corresponding flux over a shell with a radius of 500 km; (9) the maximum velocity.

phase and that BH formation may therefore be delayed or, in fact, may not occur at all for a range of putative progenitor models.³ In § 2, we present radiation hydrodynamic simulations of a collapsar-candidate model that support this thesis, using the VULCAN/2D code (Livne et al. 2004, 2007). In § 3, we discuss the implications of our results for stellar evolutionary models that might lead to collapsars and/or hypernovae.

2. MODEL AND RESULTS

We present results from two-dimensional, rotating, multi-group, flux-limited-diffusion magnetohydrodynamics simulations, using VULCAN/2D (Livne et al. 2004, 2007; see also appendices in Dessart et al. 2006 and Burrows et al. 2007a), of the 350C progenitor model and collapsar candidate of Woosley & Heger (2006, hereafter WH06). The numerical procedure that we follow is identical to that of B07 in every respect, except the choice of progenitor. WH06’s model is evolved from a $35 M_{\odot}$ zero-age main-sequence star endowed with a total angular momentum of $1.4 \times 10^{53} \text{ ergs s}$, a metallicity of 1% the solar value, and a reduction by a factor of 10 in the prescribed mass-loss rates during the Wolf-Rayet phase. Our simulations extend out to a maximum radius of 5000 km (which contains $\sim 3 M_{\odot}$) and cover a 90° quadrant, bounded by the rotation axis and the equator. We adopt WH06’s initial rota-

³ In the present context, BH formation is never prompt, since it takes a finite time, on the order of seconds, for the PNS to accumulate the critical mass at which it experiences the gravitational instability. This is in contrast with supermassive stars, such as the progenitors of pair-instability SNe, which may form an apparent horizon during collapse and thus “directly” transition to a BH (Liu et al. 2007).

tional, density, temperature, and electron-fraction profiles for that progenitor. For the magnetic field distribution, we start with magnitudes and a morphology that are consistent with the 350C model of WH06. We use a field that is uniform within 3000 km and dipolar beyond. In our reference model, M0, we employ initial poloidal and toroidal field magnitudes of 2×10^{10} and $8 \times 10^{11} \text{ G}$, respectively, in close quantitative agreement with the 350C model of WH06. However, we also study a model, M1, with an initial poloidal field that is 5 times stronger. This leads to a magnetic field energy, at $\sim 100 \text{ ms}$ after core bounce, that is closer to the value expected at the PNS surface, if we were to adequately resolve the MRI (B07).

In Table 1, we give important quantities that characterize the two simulations that were performed. Note that if magnetic fields are ignored in the precollapse evolutionary calculations of WH06, core angular velocities reach $5\text{--}22 \text{ rad s}^{-1}$, much larger than the value of 1.98 rad s^{-1} achieved in the 350C model. A bounce at subnuclear densities may ensue and may lead to BH formation (Akiyama & Wheeler 2005). Ignoring magnetic torques in the models that are most prone to magnetic field generation during the precollapse phase seems inconsistent. Thus, we focus on the more slowly rotating progenitors, which were evolved with magnetic fields and which inevitably bounce at nuclear densities.

After an initial collapse phase that lasts $\sim 245 \text{ ms}$, the central density reaches $\sim 3 \times 10^{14} \text{ g cm}^{-3}$, the EOS stiffens, and a shock is born and propagates outward, but it is debilitated by the photodissociation of the infalling outer iron core and the burst of electron neutrinos. The shock stalls at $\sim 150 \text{ km}$, and, within a few tens of milliseconds after bounce, it becomes increasingly aspherical. The net gain from neutrino emission and absorption processes, the entropy, and the material accretion rates all get progressively larger at larger latitudes as the degree of oblateness of the fast-rotating PNS increases. Subsequent to the amplification due to compression by a factor of ~ 2500 in both magnetic field components, the toroidal magnetic field increases after bounce because of the winding of the poloidal field component. At the same time, accretion of the outer magnetized core continues and enhances the total magnetic field energy. By 150 ms (300 ms) after bounce, the magnetic pressure at the surface of the PNS along the pole, in the M1 (M0) model, is comparable to the gas pressure, and a bipolar, magnetically driven, baryon-loaded, and nonrelativistic jet is initiated, reversing accretion into ejection along the polar direction. As shown in the left panel of Figure 1, the initial jet mass-loss rate is only $\sim 0.01 M_{\odot} \text{ s}^{-1}$, but, in the M1 model and by $\sim 350 \text{ ms}$ after bounce, it exceeds the accretion rate. At this time, the accumulated baryonic PNS mass is

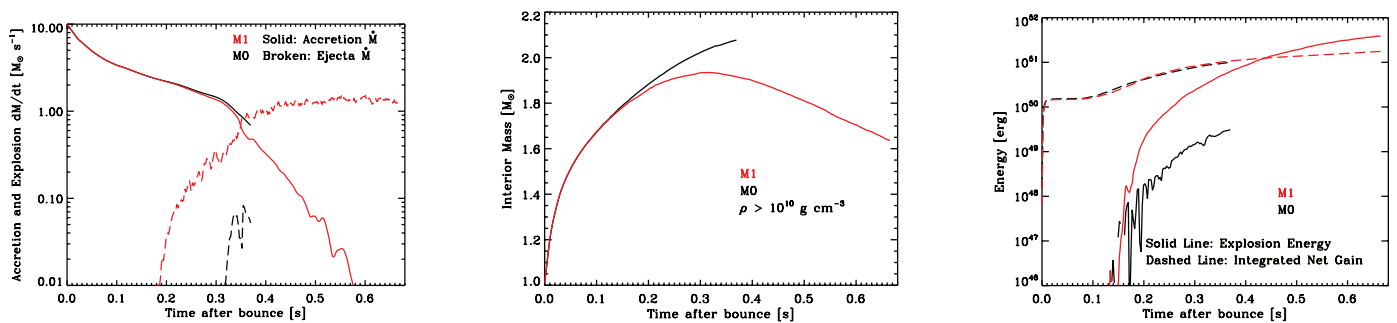


FIG. 1.—Left: Time evolution of the instantaneous integrated mass flux accreting (solid line) and outflowing (dashed lines) through a shell at a radius of 500 km, for models M0 (black lines) and M1 (red lines). Middle: Same as left, but for the total mass interior to the isodensity contour corresponding to $10^{10} \text{ g cm}^{-3}$. Right: Same as left, but for the explosion energy (solid line) and the net integrated neutrino gain (dashed lines) outside the high-density regions bounded by the $10^{10} \text{ g cm}^{-3}$ contour (see text for discussion).

only $1.93 M_{\odot}$ (middle panel of Fig. 1), and thus it is well below the $2.17 M_{\odot}$ baryonic mass transition to BH formation that we derive with our EOS (Shen et al. 1998). Note that, for a solid-body rotator, this limit may increase by up to 10%–20% (Cook et al. 1994), but, for a differentially rotating neutron star, this limit may be considerably larger (Baumgarte et al. 2000). Hence, rotation (in particular, differential rotation) enhances the potential for explosion during a PNS phase. By 650 ms after bounce, the explosion energy in the M1 model reaches $\sim 3.3 \text{ B}$ ($10^{51} \text{ ergs} \equiv 1 \text{ Bethe [1 B]}$) (see right panel of Fig. 1), although, because of the continued accretion along near-equatorial latitudes, a quasi-steady state is reached with an explosion power sustained at $\sim 10 \text{ B s}^{-1}$. As shown in Figure 2, the jet resembles a magnetic tower (Lynden-Bell 2003; Uzdensky & MacFadyen 2006) but is confined primarily by the ram pressure of the infalling dense envelope (B07). As time progresses, its base broadens, and, given the quasi-steady jet conditions, the mass ejection rate grows, and the accretion is limited to progressively smaller latitudes. The increase in ejecta volume enhances the neutrino contribution to the explosion energy, although it remains a subdominant part of the total by the end of the simulation. Extraction of core rotational energy by magnetic torques is also evident in the M1 model, from the increase in the average PNS rotation period⁴ from 8 to 12 ms between 200 and 600 ms after bounce, respectively, whereas the average period for over half this interval decreases from 5 to 4 ms in the weakly exploding M0 model. The decrease in the free energy of rotation in the M1 model is on the order of 3 B and is comparable to the magnitude of the explosion energy. This supports the idea that the core rotation energy fuels the magnetically driven ejecta. Hence, the M1 model, modified slightly to yield fields at saturation that agree roughly with what one would obtain in the presence of the MRI, boasts a clear and powerful explosion. In this model, the PNS loses mass at a steady rate, once the explosion is well established, and has a mass of only $\sim 1.7 M_{\odot}$ at the end of the simulation. The broadening of the base of the jet suggests that the explosion will not choke (or induce any significant fallback) but, instead, by encompassing a larger solid angle, will lead to an explosion in all directions. Hence, such an object is unlikely to transition to a BH or to lead to a collapsar.

By contrast, in the M0 model, the explosion happens later, when the neutron star baryonic mass has already accumulated $\sim 2.1 M_{\odot}$, and thence may be susceptible to collapsing into a BH. The free energy of the core rotation has been partially tapped, but the potential subsequent powering of a GRB may not be compromised. This model, by mimicking more slowly rotating cores or an inefficient MRI, offers a limiting case for the formation or nonformation of a BH and a possible collapsar.

3. DISCUSSION

The potential for exponential growth on a rotational timescale of initial seed magnetic fields by the MRI (Shibata et al. 2006; Etienne et al. 2006), fueled by the free energy of core rotation, makes the initial angular momentum budget of the progenitor star the key parameter in determining the outcome during the immediate postbounce phase (B07). A magnetically driven, baryon-loaded, and nonrelativistic explosion is obtained for WH06's 35OC collapsar candidate model, which was evolved at low metallicity from a $35 M_{\odot}$ fast-rotating main-sequence star. The explosion occurs $\sim 200 \text{ ms}$ after bounce and reaches $\sim 3 \text{ B}$ $\sim 400 \text{ ms}$ later. After an initial accretion phase, the steadily decreasing PNS

⁴ We define the average rotation period as the period of the rigidly rotating PNS that has the same total angular momentum and structure inside the $10^{10} \text{ g cm}^{-3}$ isodensity contour.

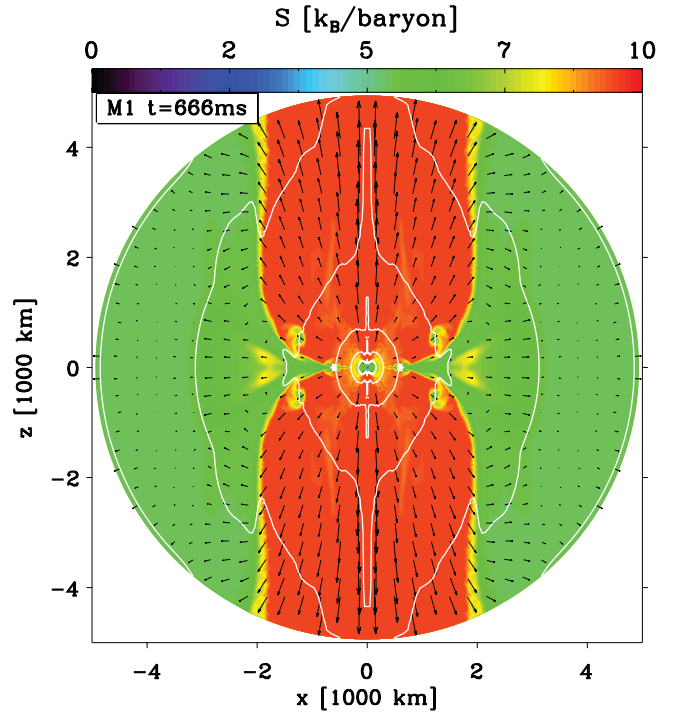


FIG. 2.—Color map of the entropy at 666 ms after bounce for model M1, overlaid with white isodensity contours (every decade downward from $10^{10} \text{ g cm}^{-3}$) and velocity vectors (length saturated to 15% of the width of the display and corresponding to a velocity of $30,000 \text{ km s}^{-1}$).

mass reaches only $\sim 1.7 M_{\odot}$ at the end of the simulation, and thus the quasi-steady explosion we observe suggests that BH formation is unlikely to occur. Moreover, baryon contamination prevents the ejecta from becoming relativistic. Note that the production of a GRB in the collapsar context is contingent on the gravitational collapse of the PNS into a BH.

The recent stellar evolutionary calculations by Yoon & Langer (2005), WH06, and Meynet & Maeder (2007) of fast-rotating main-sequence objects at low metallicity systematically predict such fast-rotating cores at collapse. Starting from similar conditions for a $35\text{--}40 M_{\odot}$ star but using different mass-loss “recipes,” they obtain very similar rotational profiles in the inner core. Allowing for anisotropic mass loss (Meynet & Maeder 2007), a model by C. Georgy (2007, private communication) suggests an even larger (by a factor of 2) specific angular momentum in the inner $3 M_{\odot}$ at the end of silicon core burning. Despite the agreement between these different evolutionary computations, the magnetically driven explosion and the “failed” BH formation described here are conditional on the uncertain treatment of mass loss, angular momentum transport, and magnetic processes (Spruit 2002) during the precollapse evolution.

At very low metallicities, radiatively driven winds of massive stars are inhibited by the lack of metals (Kudritzki 2002; Vink et al. 2001; Vink & de Koter 2005), whose optically thick lines intercept radiation momentum (Castor et al. 1975). Recent downward revisions of mass-loss rates due to clumping (Owocki et al. 1988; Bouret et al. 2005; Fullerton et al. 2006) suggest, however, the potential importance of episodic outbursts, akin to the 1843 giant eruption of η Carina (Smith & Owocki 2006). The metallicity dependence of such phenomena is entirely unknown, mostly because the fundamental cause of the outburst remains a mystery. While line driving seems to be excluded, continuum driving of a porous medium at super-Eddington luminosities has been proposed by

Owocki et al. (2004) as an alternative. Finally, mass loss in fast-rotating, and sometimes critically rotating (Townsend et al. 2004), envelopes is complicated by the effects associated with centrifugal support, surface oblateness, and gravity darkening (Cranmer & Owocki 1995; Owocki et al. 1996), so that the mass-loss “recipes” used in stellar evolutionary models are not always substantiated by observational or theoretical evidence. At present, and in light of our simulations, it appears that the chemically homogeneous evolution of fast-rotating main-sequence massive stars at low metallicity systematically yields iron cores at collapse that may have *too much* angular momentum, a property that prevents the formation of a collapsar. Uncertainties in the modeling of the precollapse evolution may result, however, in slower rotating iron cores and, thus, might inhibit an early magnetically driven explosion in favor of a black hole, and perhaps collapsar, formation.

We conclude that variations in the angular momentum distribution of precollapse massive stars may lead to different postbounce scenarios. Nonrotating or slowly rotating progenitors may explode with weak/moderate energy (≤ 1 B) through a neutrino or an acoustic mechanism ≤ 1 s after bounce, or they may collapse into a BH. Objects with large angular momentum in the envelope but little in the core may proceed through the PNS phase, transition to a BH, and form a collapsar with a GRB signature. Owing to the modest magnetic field amplification above the PNS, a weak precursor polar jet may be launched but may soon be overtaken by a baryon-free, collimated relativistic jet. At the same time, the progenitor envelope is exploded by a disk wind, resulting in a hypernova-like SN with a large luminosity (large ^{56}Ni mass). Finally, we conclude that objects with large angular momentum in the core may not transition to a BH. Instead, fueled by core-rotation energy, a magnetically driven, baryon-loaded, nonrelativistic jet is obtained without any GRB signature. The explosion has

the potential of reaching energies of a few to 10 B, and for observations along the poles, this explosion may look like a Type Ic hypernova-like SN with broad lines. For an observation at lower latitudes, the delayed and less energetic explosion nearer the equator may look more like a standard Type Ic SN (Höflich et al. 1999). This volume-restricted jetlike explosion is dimmer, as the amount of processed ^{56}Ni may be significantly less than the $\sim 0.5 M_{\odot}$ obtained in the collapsar context (MacFadyen & Woosley 1999). Hence, magnetic processes during the postbounce phase of fast-rotating iron cores offer a potential alternative to collapsar formation and long-soft GRBs by producing nonrelativistic, non-Poynting-flux-dominated baryon-loaded hypernova-like explosions without any GRB signature. Importantly, while our study narrows the range over which the collapsar model may exist, it also offers additional routes to explain the existence of GRB/SN-hypernova events, like SN 1998bw (Woosley et al. 1999), and hypernova events, like SN 2002ap, without a GRB signature (Mazzali et al. 2002).

More generally, magnetic effects should naturally arise in the context of gravitational collapse and fast rotation. The resulting angular momentum of newly formed BHs and magnetars, for example, would be reduced, perhaps considerably, by any prior magnetically driven explosion and, thus, may decrease the power of subsequent mass ejections from compact objects (see, e.g., Thompson et al. 2004).

We acknowledge support for this work from the Scientific Discovery through Advanced Computing (SciDAC) program of the DOE, under grants DE-FC02-01ER41184 and DE-FC02-06ER41452, and from the NSF, under grant AST-0504947. E. L. thanks the Israel Science Foundation for support under grant 805/04, and C. D. O. thanks the Joint Institute for Nuclear Astrophysics (JINA) for support under NSF grant PHY0216783.

REFERENCES

- Akiyama, S., & Wheeler, J. C. 2005, *ApJ*, 629, 414
Akiyama, S., et al. 2003, *ApJ*, 584, 954
Aloy, M. A., Müller, E., Ibáñez, J. M., Martí, J. M., & MacFadyen, A. 2000, *ApJ*, 531, L119
Ardeljan, N. V., et al. 2005, *MNRAS*, 359, 333
Balbus, S. A., & Hawley, J. F. 1991, *ApJ*, 376, 214
Baumgarte, T. W., et al. 2000, *ApJ*, 528, L29
Bouret, J. C., Lanz, T., & Hillier, D. J. 2005, *A&A*, 438, 301
Buras, R., Rampp, M., Janka, H.-T., & Kifonidis, K. 2006, *A&A*, 447, 1049
Burrows, A., et al. 2006, *ApJ*, 640, 878
———. 2007a, *ApJ*, 655, 416
———. 2007b, *ApJ*, 664, 416 (B07)
Castor, J. I., Abbott, D. C., & Klein, R. I. 1975, *ApJ*, 195, 157
Cook, G. B., et al. 1994, *ApJ*, 424, 823
Cranmer, S. R., & Owocki, S. P. 1995, *ApJ*, 440, 308
Dessart, L., Burrows, A., Livne, E., & Ott, C. 2006, *ApJ*, 645, 534
———. 2007, *ApJ*, 669, 585
Etienne, Z. B., Lui, Y. T., & Shapiro, S. L. 2006, *Phys. Rev. D*, 74, 044030
Fullerton, A. W., et al. 2006, *ApJ*, 637, 1025
Hjorth, J., et al. 2003, *Nature*, 423, 847
Höflich, P., Wheeler, J. C., & Wang, L. 1999, *ApJ*, 521, 179
Iwamoto, K., et al. 1998, *Nature*, 395, 672
Kitaura, F. S., et al. 2006, *A&A*, 450, 345
Kotake, K., Sawai, H., Yamada, S., & Sato, K. 2004, *ApJ*, 608, 391
Kudritzki, R. P. 2002, *ApJ*, 577, 389
Liu, Y. T., Shapiro, S. L., & Stephens, B. C. 2007, *Phys. Rev. D*, 76, 084017
Livne, E. et al. 2004, *ApJ*, 609, 277
———. 2007, *ApJS*, 170, 187
Lynden-Bell, D. 2003, *MNRAS*, 341, 1360
MacFadyen, A. I., & Woosley, S. E. 1999, *ApJ*, 524, 262
MacFadyen, A. I., Woosley, S. E., & Heger, A. 2001, *ApJ*, 550, 410
Marek, A., & Janka, H.-T. 2007, *ApJ*, submitted (astro-ph/0708.3372)
Mazzali, P. A., et al. 2002, *ApJ*, 572, L61
Meynet, G., & Maeder, A. 2007, *A&A*, 464, L11
Moiseenko, S. G., et al. 2006, *MNRAS*, 370, 501
Obergaulinger, M., Aloy, M. A., & Müller, E. 2006, *A&A*, 450, 1107
Ott, C. D., et al. 2006, *ApJS*, 164, 130
Owocki, S. P., Castor, J. I., & Rybicki, G. B. 1988, *ApJ*, 335, 914
Owocki, S. P., Cranmer, S. R., & Gayley, K. G. 1996, *ApJ*, 472, L115
Owocki, S. P., Gayley, K. G., & Shaviv, N. J. 2004, *ApJ*, 616, 525
Pessah, M. E., Chan, C.-K., & Psaltis, D. 2006, *MNRAS*, 372, 183
Proga, D. 2005, *ApJ*, 629, 397
Sawai, H., Kotake, K., & Yamada, S. 2005, *ApJ*, 631, 446
Shen, H., Toki, H., Oyamatsu, K., & Sumiyoshi, K. 1998, in *Neutron Stars and Pulsars: Thirty Years after the Discovery*, ed. N. Shibasaki (Tokyo: Universal Academy Press), 157
Shibata, M., Liu, Y. T., Shapiro, S. L., & Stephens, B. C. 2006, *Phys. Rev. D*, 74, 104026
Smith, N., & Owocki, S. P. 2006, *ApJ*, 645, L45
Sprit, H. C. 2002, *A&A*, 381, 923
Stanek, K. Z., et al. 2003, *ApJ*, 591, L17
Thompson, T. A., Chang, P., & Quataert, E. 2004, *ApJ*, 611, 380
Townsend, R. H. D., et al. 2004, *MNRAS*, 350, 189
Uzdensky, D. A., & MacFadyen, A. I. 2006, *ApJ*, 647, 1192
Vink, J. S., & de Koter, A. 2005, *A&A*, 442, 587
Vink, J. S., et al. 2001, *A&A*, 369, 574
Wheeler, J. C., Meier, D. L., & Wilson, J. R. 2002, *ApJ*, 568, 807
Wheeler, J. C., Yi, I., Höflich, P., & Wang, L. 2000, *ApJ*, 537, 810
Woosley, S. E. 1993, *ApJ*, 405, 273
Woosley, S. E., & Bloom, J. S. 2006, *ARA&A*, 44, 507
Woosley, S. E., & Heger, A. 2006, *ApJ*, 637, 914 (WH06)
Woosley, S. E., et al. 1999, *ApJ*, 516, 788
Yamada, S., & Sawai, H. 2004, *ApJ*, 608, 907
Yoon, S.-C., & Langer, N. 2005, *A&A*, 443, 643
Zhang, W., Woosley, S. E., & MacFadyen, A. I. 2003, *ApJ*, 586, 356